

Very large rain drops from 2D video disdrometers and concomitant polarimetric radar observations

Merhala Thurai¹, Patrick Gatlin^{2,3}, V.N. Bringi¹ and Lawrence Carey²

¹*Dept. of ECE, Colorado State University, Fort Collins, Colorado 80523, United States*

²*University of Alabama, Huntsville, United States*

³*NASA Marshall Space Flight Center, Huntsville, United States*

(Dated: 17 July 2014)



1 Introduction

Drop size distribution (DSD) measurements using ground-based disdrometers (point measurements) have often been used to derive equations to relate radar observations to the integral rainfall parameters (Atlas et al. 1999, Bringi et al., 2003, Kozu et al., 2006, Tokay and Short, 1996, Ajayi and Owolabi, 1987, Battan, 1973). Disdrometers such as JWD, MRR and several others have a major limitation in measuring drops with equi-volume diameters (D_{eq}) larger than 5 mm because they often rely on the velocity-diameter relationship which plateaus beyond this diameter range (Atlas et al., 1973, Gunn & Kinzer, 1949). Other disdrometers such as Parsivel also lack accuracy beyond this diameter range. The 2D video disdrometer (2DVD; Schönhuber et al., 2008) on the other hand gives drop-shape contours and velocities for each individual drop/hydrometeor falling through its sensor area; this provides a unique opportunity to study the role of very-large drops on radar measurements in particular those with polarimetric radar capability where DSDs with a significant component of very large drops may require special consideration given that the differential reflectivity and other polarimetric radar parameters including attenuation-correction methods will be sensitive to the concentrations of these large drops.

A recent study on the occurrence of large drops by Gatlin et al. (2014) has compiled a large and diverse set of measurements made with the 2D video disdrometers from many locations around the globe. Some of the largest drops found in this study were 9 mm D_{eq} and larger, and in this paper, we report on three such events, with maximum D_{eq} 's of 9.0, 9.1 and 9.7 mm, which occurred in Colorado, Northern Alabama, and Oklahoma, respectively. Detailed examination of the 2DVD data – in terms of shapes and fall velocities – has confirmed that these are fully-melted hydrometeors, although for the last case in Oklahoma, a bigger and non-fully-melted hydrometeor was also observed. All three events were also captured by polarimetric radars, namely the S-band CHILL radar operated by Colorado State University (Brunkow et al., 2000), the C-band ARMOR radar (Petersen et al., 2007) operated by University of Alabama in Huntsville, and NEXRAD-KVNX, operated by the US National Weather Service, respectively. For the last event, several other radar observations were also made, including two X-band radars operated by the US Dept. of Energy.

Analyses of 2DVD data in conjunction with the corresponding radar observations are presented, along with some discussion on sampling issues related to the measurements of such large rain drops. The latter is addressed using maximum diameter D_{max} measurements from 1-minute DSDs using two collocated 2DVDs for 37 events in Huntsville.

2 The three events

2.1 The Colorado event

This event occurred on Sept. 10 2006 and was captured both by a 2DVD unit located near the town of Platteville and the CHILL radar ~30 km away which performed a predefined series of scans that included some 'fixed pointing' (dwell mode, along the azimuth of the 2DVD site, with low elevation angle) and RHI scans over Platteville as well as a few interlaced PPI scans. Weather reports during this event had reported thunderstorm activity associated with this event. The radiosonde data collected at 00 UTC 11 September 2006 sounding from Denver, Colorado, indicated that relatively moist conditions were present between the 700 and 240 mb levels (corresponding to 3.14 and 10.97 km a.s.l.); this sounding contained ~1.9 cm of precipitable water which is a little higher than normal for September in Colorado.

The PPI scans showed an isolated and intense rain cell with 50 dBZ reflectivity and 4 dB differential reflectivity, while the low values of hail detection ratio ($HDR < 0$ dB) suggested that it was all fully-melted hydrometeors, at least near the ground. One of the RHI scans is shown in Fig. 1. Both reflectivity and the linear depolarization ratio (LDR) are given. The intense, isolated cell can be seen over the 2DVD site at 30 km range. The cell is detached from another more widespread system which can be seen at closer ranges (up to 15 km). The melting layer is clearly visible for this widespread system, particularly in LDR at a height around 2 km. By comparison, LDR values within the intense isolated cell are very low (< -28 dB), indicating that there was no hail aloft. (Unfortunately, due to another project commitment, the radar was transmitting only H polarization for RHI scans – but H & V on receive).

In the fixed pointing and PPI modes, all polarization parameters were recorded. An example of a PPI scan taken 21 minutes earlier is shown in Fig. 2. The isolated cell can be seen a few km away at this time from the 2DVD site. The reflectivity values can be seen (once again) to be more than 50 dBZ and Z_{dr} values reaching 5 dB and higher, indicating the

presence of very large drops. The S-band hail detection ratio ($HDR < 0$ dB) indicates that this rain cell is composed of fully-melted raindrops, also confirmed by high specific differential propagation phase shift (K_{dp}) values (not shown here). The isolated cell reaches an altitude of nearly 10 km with echo-top reflectivities around 0 dBZ at these heights.

Fig. 1: RHI scans of Z and LDR recorded by the CSU-CHILL radar over the 2DVD site at Platteville (30.4 km range) on 10 Sept 2006 when large drops were recorded by the 2DVD. Scan time is: 22:28 UTC. The biggest drop was 9 mm (fully-melted) for this event.

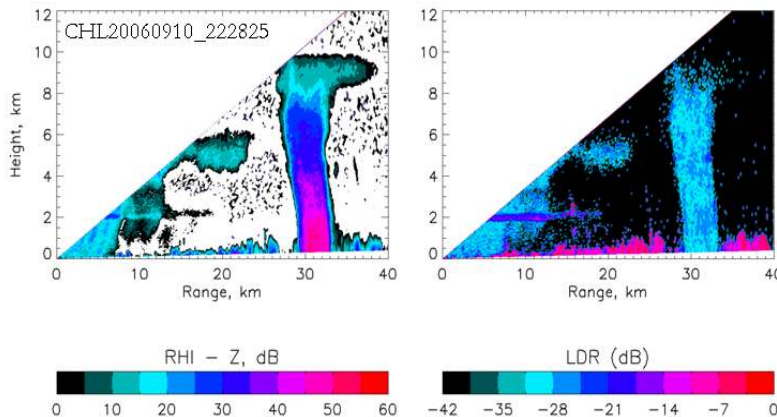
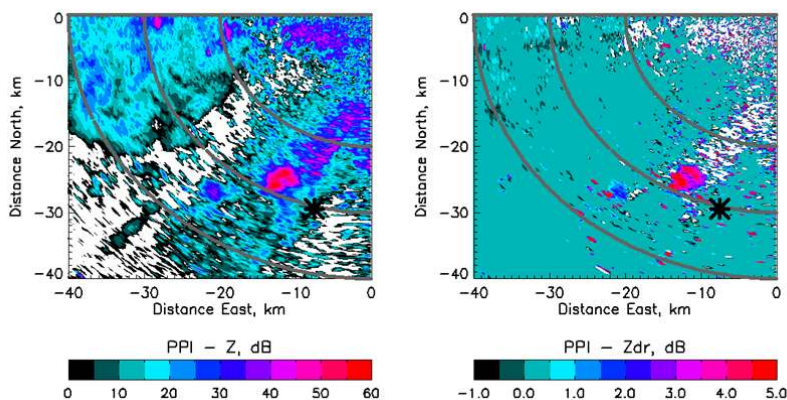
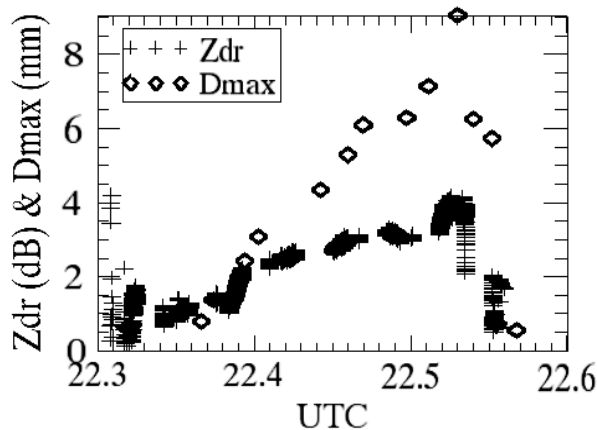


Fig. 2: A PPI sector scan for the same event as Fig. 1 but taken earlier at 22:07 UTC. The 2DVD location is marked with a black star.



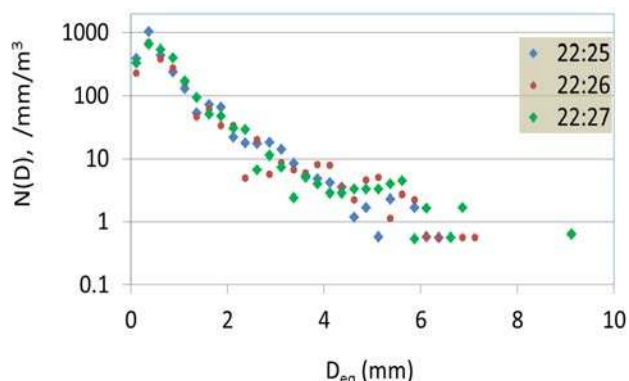
Using the radar data collected in the fixed, pointing dwell mode, it was possible to extract Z_{dr} over the 2DVD site and correlate with D_{max} from the 2DVD 1-minute DSD measurements. Fig. 3 shows this comparison from 22:18 to 22:36 UTC. Just after 22:30 UTC, the 9 mm D_{max} can be seen and it is around this time that the Z_{dr} reaches its highest value of ~ 4 dB. T-matrix calculations using the measured 1-minute DSDs also resulted in Z_{dr} near 4 dB. At C-band, the T-matrix calculations yielded Z_{dr} as high as 6.5 dB (due to non-Rayleigh scattering effects), whereas at X-band and Ku-band, Z_{dr} values of 4 dB and 3.4 dB were obtained. This clearly shows the importance of D_{max} particularly for Z_{dr} at C-band.

Fig. 3: Z_{dr} extracted over the 2DVD site (after smoothing in range) as time series from the CHILL radar fixed pointing measurements and D_{max} recorded by the 2DVD at ground level.



The 1-minute DSD during which the 9 mm drop was detected consisted of only drops with $D_{eq} \leq 7$ mm except for the one single drop with $D_{eq} = 9.0$ mm. Fig. 4 shows three 1-minute consecutive DSDs around this period. The variability of DSD is not all that significant for diameters less than 7 mm. Clearly, sampling issues need to be considered when determining D_{max} for scattering calculations. The importance of D_{max} , particularly for Z_{dr} at C-band, has also been shown by Keenan et al. (2001) and Carey and Petersen (2014).

Fig. 4: Consecutive 1-minute DSDs during the 9 mm drop event.



In Table 1 we show the effect of neglecting the 9 mm drop on the radar parameters at S, C and X bands. T-matrix calculations were performed assuming identical values for parameters such as temperature, shape-size relation and orientation angle distribution. Some differences are seen in Z_h , Z_{dr} and K_{dp} (with and without the 9 mm drop). In general, they show somewhat reduced values when the 9 mm drop is excluded, except for Z_{dr} at C-band which shows an increase which can be attributed to the non-Rayleigh scattering effects (resonance) which peaks around 6 mm for Z_{dr} at C-band. Also included in Table 1 are the values of D_m and σ_M (the mass-weighted mean diameter and the standard deviation of the mass spectrum respectively) for the same DSD with and without the 9 mm drop. A 7% reduction is seen in D_m and a 15% reduction in σ_M .

Table 1: The effect of including (with) and excluding (without) the 9 mm drop on the radar parameters at various frequency bands. The assumptions are: Temperature = 22 °C, std. dev. (canting angle) = 5 deg., and oblate spheroid shapes for drops with axis ratios given in eq. (2) of Thurai et al. (2007).

	Z_h (dBz)	Z_{dr} (dB)	K_{dp} (deg/km)
S-band (with)	53.6	4.0	1.5
S-band (without)	53.4	3.7	1.3
C-band (with)	57.6	5.5	2.6
C-band (without)	56.8	5.9	2.1
X-band (with)	56.5	3.9	3.5
X-band (without)	56.8	3.7	3.9
D_m (with) = 4.36 mm D_m (without) = 4.05 mm			
σ_M (with) = 2.17 mm σ_M (without) = 1.85 mm			

2.2 The Oklahoma event

In the study by Gatlin et al. (2014) using global 2DVD datasets, the very large drops - exceeding 8 mm D_{eq} - were found in both tropical and mid-latitude locations. The greatest number of giant raindrops were found in the mid-latitudes, with the largest being a 9.7 mm raindrop that occurred in northern Oklahoma during the passage of a hail producing thunderstorm. The results suggested that the very large raindrops are more likely to fall from clouds that contain hail, especially those raindrops exceeding 8 mm in diameter.

The event with the biggest raindrop (D_{eq} of 9.7 mm as mentioned earlier) was observed in northern Oklahoma at the Atmospheric Radiation Measurement Central Facility (ARM-CF) site operated by the U.S. Department of Energy (DoE). A reconstructed three dimensional image of this giant raindrop, which was recorded by the DoE's compact-version of 2DVD,

is shown in Fig. 5. The shape of the 9.7 mm raindrop is very similar to the raindrop shape contours computed by Thurai et al. (2007) (However, note the term c_4 in equation (1) of this reference needs adjustment for $D_{eq} > 7.5$ mm). The raindrop was produced by a left-moving supercell storm, which is commonly known to be a large hail-bearing type of storm (Bunkers 2000), that occurred during the overnight hours of April 29, 2012. The 2DVD also recorded some melting hail, similar in shape to that described by Rasmussen et al. (1984), as this storm passed over the site. Thus the existence of a small ice core within this 9.7 mm hydrometeor cannot be ruled out, but is very unlikely given its shape (Fig. 5). Furthermore, one minute prior to when the 9.7 mm raindrop was recorded, dual-polarimetric measurements from the Vance, OK NEXRAD radar, which is located about 55 km away, indicate that the precipitation over the ARM Central Facility was dominated by high Z_{dr} around 3-4 dB, K_{dp} of 3° km^{-1} and $HDR \ll 0$ dB, similar to the CHILL radar measurements of the event which produced the 9.0 mm raindrop presented in section 2.1.

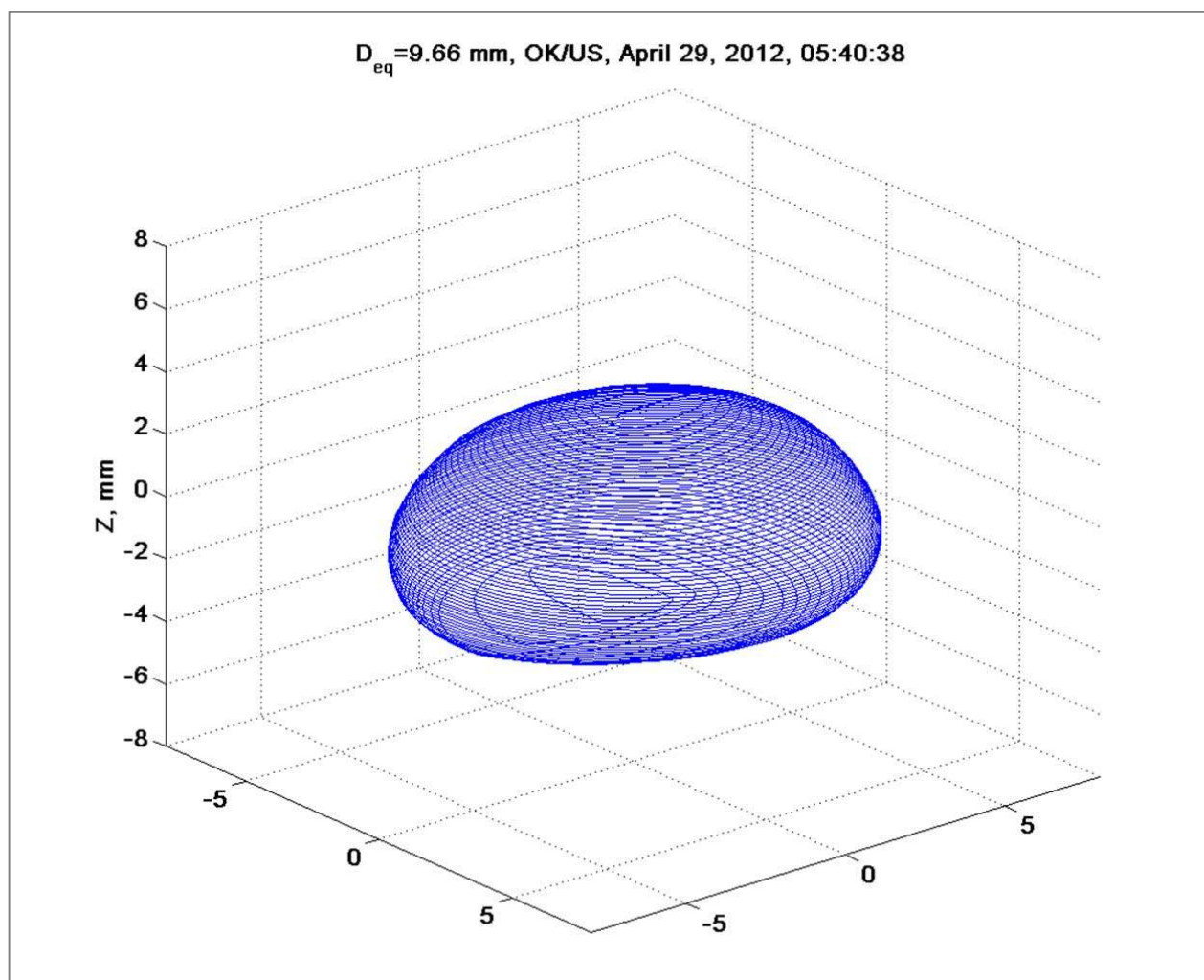
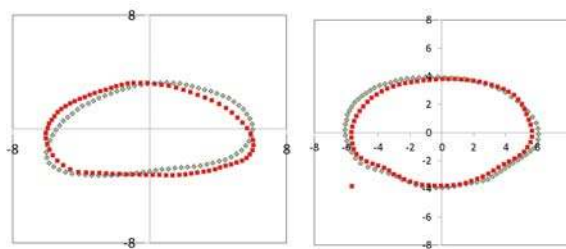


Fig. 5: A three-dimensional reconstruction of the 9.7 mm raindrop that was recorded by the DOE's 2DVD at their ARM Central Facility site in Oklahoma on April 29, 2012 at 05:38:53 UTC. This is the biggest drop (fully melted) recorded to date. X, Y and Z dimensions are in mm. A well known fact is that any drop with D_{eq} even a little bit larger than this will become aerodynamically unstable resulting in spontaneous drop break-up.

As mentioned earlier, the 2DVD at the SGP-CF did measure some non-fully melted hydrometeors during this event. The contours of the projected silhouettes onto the two orthogonal planes are shown in Fig. 6 for (a) the 9.7 mm drop corresponding to Fig. 5 and (b) a larger hydrometeor which is not fully melted. The differences in the two sets of images are obvious. In the case of the unmelted hydrometeor it is evident that it does not possess the flattened base as predicted for example by the Beard-Chuang (1986) model and instead shows some irregularities/discontinuities near the base and more flatted shape at the top.

Fig 6: The silhouette contours from the 2DVD of (a) the largest, fully melted, drop shown in Fig. 5 and (b) a larger, non-fully melted, hydrometeor. X/Y and Z dimensions are in mm.



A PPI sector scan taken from the Vance OK NEXRAD (KVNx) is shown in Fig. 7. The time of the scan is 05:41:42 UTC—a few minutes *after* the largest drop was recorded. The black square indicates the 2DVD location. High Z , Z_{dr} and K_{dp} values are seen around this location indicating that it is mostly due to rain although the lower than expected ρ_{hv} values (at S-band) also suggest the possibility of graupel/hail mixture. High values of HDR can be seen some 5-10 km west of the 2DVD site, indicating high probability of graupel/hail contamination in this region. Also shown – as a pink diamond – is the location of an X-band radar (belonging to US Dept. of Energy) at Garber which also captured this event. The Garber radar data are shown in Fig. 8, together with the estimated rainfall rate. Because of the higher radar range resolution (50 m) and the closer range, the X-band data show finer details of the storm structure. At 5:40 UTC, the Garber radar shows the core of left-moving cell is over the 2DVD site. The larger drops are associated with the sharp edge of the storm.

By comparing Fig. 7 and Fig. 8, the following observations can be made: (a) Z_h and Z_{dr} at S and X band are somewhat similar in the regions around the 2DVD location (attenuation correction schemes have been applied); (b) K_{dp} is significantly higher at X-band; (c) K_{dp} based rainfall rates at S and X bands give similar values and in fact, at the location of the 2DVD, they also agree well with the 2DVD-based estimate (~ 80 mm/h at the time of the PPI scans).

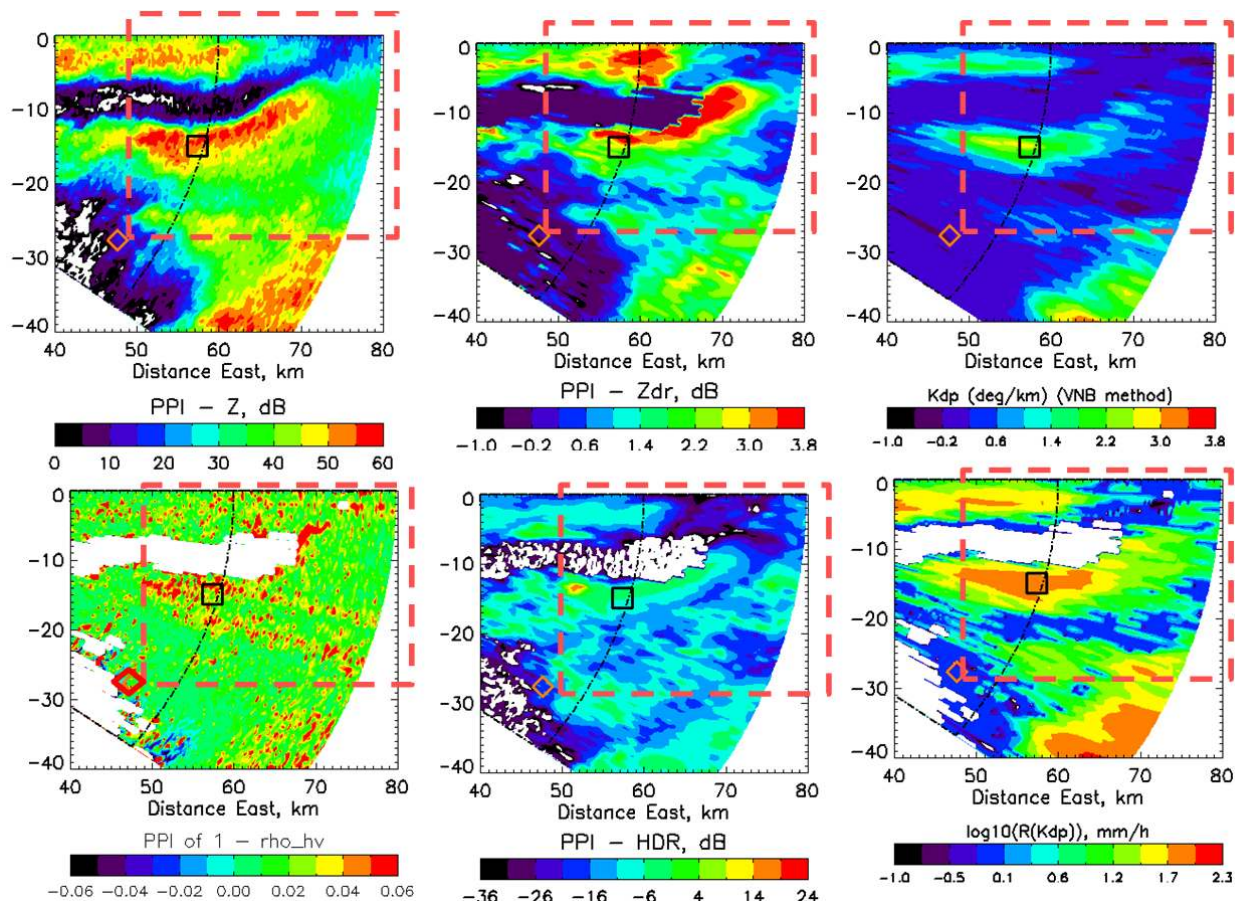


Fig. 7: Sector (SE) of PPI scan (S-band) taken at 05:41:42 UTC, a few minutes after the biggest drop was recorded by the 2DVD. The location of the 2DVD is marked with a black square. The top three panels are Z_h , Z_{dr} , and K_{dp} , and the bottom panels are $1-\rho_{hv}$, HDR and rainfall rate estimated from K_{dp} . The pink diamond shows the location of the Garber X-band radar and the pink dashed line represents the area of the sector corresponding to Fig. 8.

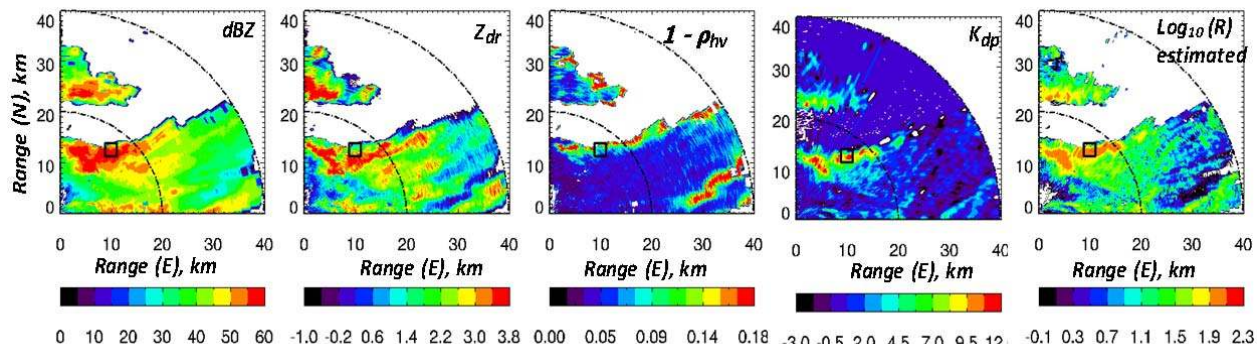


Fig. 8: A PPI sector scan (X-band) taken at 05:40 UTC, a few minutes after the biggest drop was recorded by the 2DVD. The black square marks the location of the 2DVD. The panels from right to left are Z_h , Z_{dr} , K_{dp} , $1-\rho_{hv}$, and $\log_{10}(R(K_{dp}))$ in mm/h.

The similarity between S-band Z_{dr} and X-band Z_{dr} can also be corroborated by 2DVD data. Fig. 9(a) shows the variation of D_m versus Z_{dr} at S and X bands calculated using the 1-minute DSDs from the 2DVD measurements for this event. The variation is not very different between the two. Fig. 9(b) shows K_{dp} versus rainfall rate using the same DSDs, and as observed earlier (see point (b) above), the X-band K_{dp} values are significantly higher than those at S-band. For 30 mm/h rainfall rate, the S-band K_{dp} is typically around 0.6 deg/km compared with ~ 2.65 deg/km at X-band. For 100 mm/h, they are ~ 2.3 and 8.3 deg/km respectively. Matrosov et al. (2006) have also shown similar values (ratio of 3.6 for 33 mm/h rainfall rate for K_{dp} at X-band to S-band, but it should be noted that the ratios are sensitive to drop shapes).

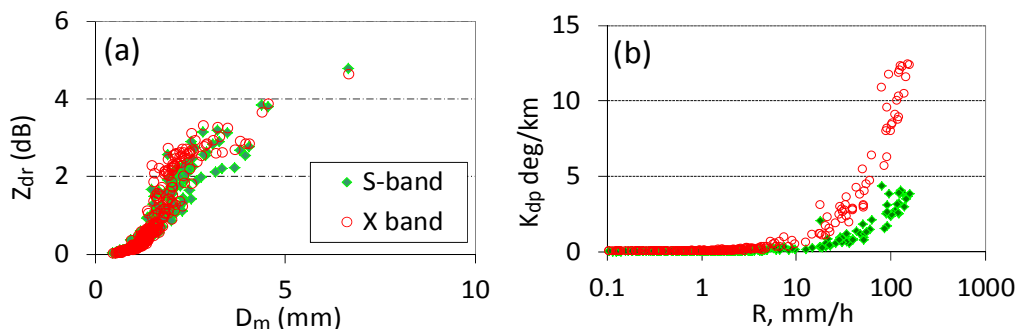
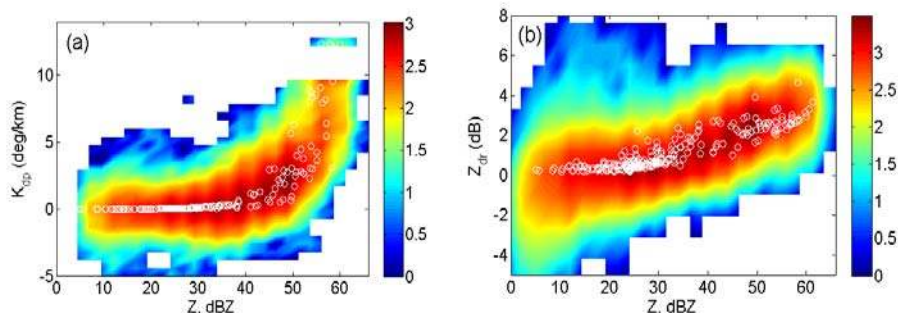


Fig. 9: (a) Z_{dr} versus D_m and (b) K_{dp} versus R , calculated using the measured 1-minute DSDs for S and X bands.

Further comparisons between the Gerber radar observations and the 2DVD based calculations are shown in Fig. 10 in terms of (a) K_{dp} versus Z_h variation and (b) Z_{dr} versus Z_h variation. In both cases, the color intensity plot represents those determined from the radar data (after correcting for attenuation) while the white circles represent the scattering calculations using the 1-minute DSDs measured by the 2DVD for this event. Note significant offsets needed to be applied to both the Gerber radar measured Z_h and Z_{dr} to get consistency with the 2DVD based variations.

Fig. 10: K_{dp} versus Z_h and Z_{dr} versus Z_h from the Garber X-band radar data (color) after applying calibration offsets and attenuation correction schemes compared with 2DVD based calculations (white dots).



2.3 Huntsville event

Another raindrop exceeding 9 mm in diameter found in the datasets was recorded by CSU's low-profile 2DVD (SN16) in Huntsville, Alabama, on March 5, 2013 at 17:56 UTC. This raindrop had a $D_{eq} = 9.1$ mm and was also produced by a storm that resulted in several reports of 2.5 cm hail at the ground shortly after it moved across the Huntsville area. Although it was a rain dominated event, the quick-look 2DVD images did indeed show the presence of (somewhat) irregular shapes. One example is shown in Fig. 11 which contrasts the 9.1 mm fully melted drop with a larger hydrometeor perhaps with melting occurring around the 'equator' of the particle (presumably wet-ice). Whether such particles can cause much higher differential attenuation or not can only be established with scattering calculations using methods which are capable of utilizing the full-3D structure of the hydrometeors including details of the complex permittivity. A fast and efficient method is the higher order method-of-moments surface integral equation technique (MoM-SIE, see Notaros, 2008) which has already been used for scattering matrix calculations for raindrops with no rotational symmetry axis (such as those immediately after a collision process) by Sekeljic et al. (2014) and Thurai et al. (2014).

Fig. 11: The two contoured silhouettes from the two orthogonal cameras of (a) the 9.1 mm drop and (b) a non-fully-melted hydrometeor from the Huntsville event on 05 Mar 2013.

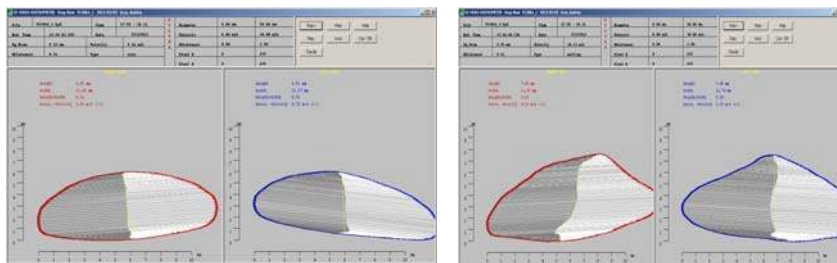


Fig. 12 shows the rainfall rate (R) as well as the DSD characteristics of this event from the 2DVD measurements – assuming all fully melted hydrometeors – a reasonable assumption given that this event was indeed dominated by rain. 3-minute running averaged values are shown. At 17:56 UTC, i.e. when the 9.1 mm drop was recorded, D_m values reach just over 3 mm, σ_M reach around 2 mm and rainfall rate is around 20 mm/h.

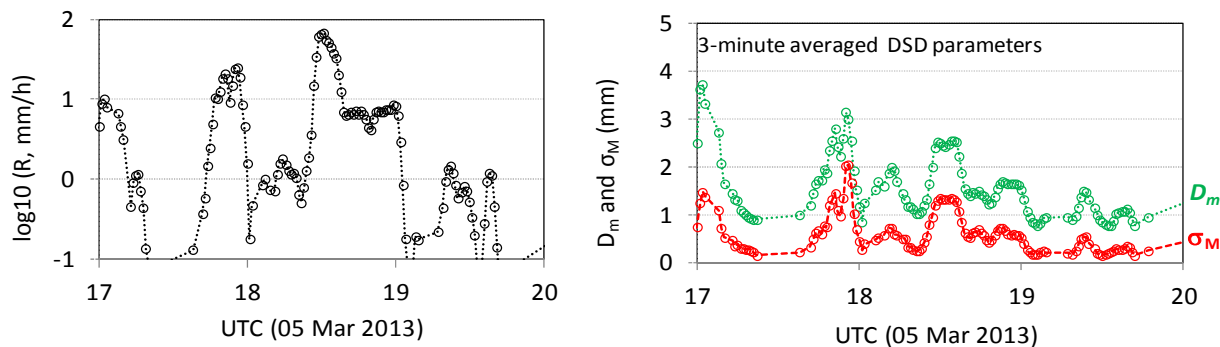


Fig. 12: R (left panel) and D_m and σ_M (right panel) from the 2DVD measured DSDs (3-min running average is applied).

The wide DSDs with the very large drops will be expected to give rise to not only high Z_{dr} at C-band but also significantly reduced ρ_{hv} and also finite (detectable) values of differential backscatter phase. Fig. 13 shows the C-band ARMOR radar scans taken at 17:54 UTC – two minutes prior to the 9.1 mm drop measurement. The 2DVD site is marked with a square. The top panels show – from left to right – Z , Z_{dr} , K_{dp} and $1-\rho_{hv}$. The Z_{dr} values reach over 8 dB (to be expected at C-band with such large drops) and ρ_{hv} shows noticeable reduction. In fact, it has been shown that the reduced ρ_{hv} at C-band can be used to determine the σ_M for wide DSDs (e.g., Thurai et al. 2008). The lower panels show – from left to right – the differential backscatter phase (δ), D_m determined from Z_{dr} , σ_M determined from $1-\rho_{hv}$ and Z_{dr} (using the method described in Thurai et al., 2008) and rainfall rate estimated from K_{dp} . The estimated DSD parameters, D_m and σ_M show good agreement with the 2DVD based estimates shown in Fig. 12 at 17:56 UTC (around 3 mm and 2 mm, respectively). Note also that significant δ can be seen in Fig. 13 indicating the presence of large drops (but perhaps also mixed with a small fraction of partially melting graupel/hail). For rain-only medium, it would be possible to include δ to further improve the DSD retrieval at C-band, as was done at X-band by Otto and Russchenberg (2010). Moreover, simulations by Bringi et al. (1991) at C-band have shown a monotonic and rapid increase of δ with Z_{dr} for $Z_{dr} > 2$ dB at C-band which clearly indicates the added advantage of including δ in DSD retrievals.

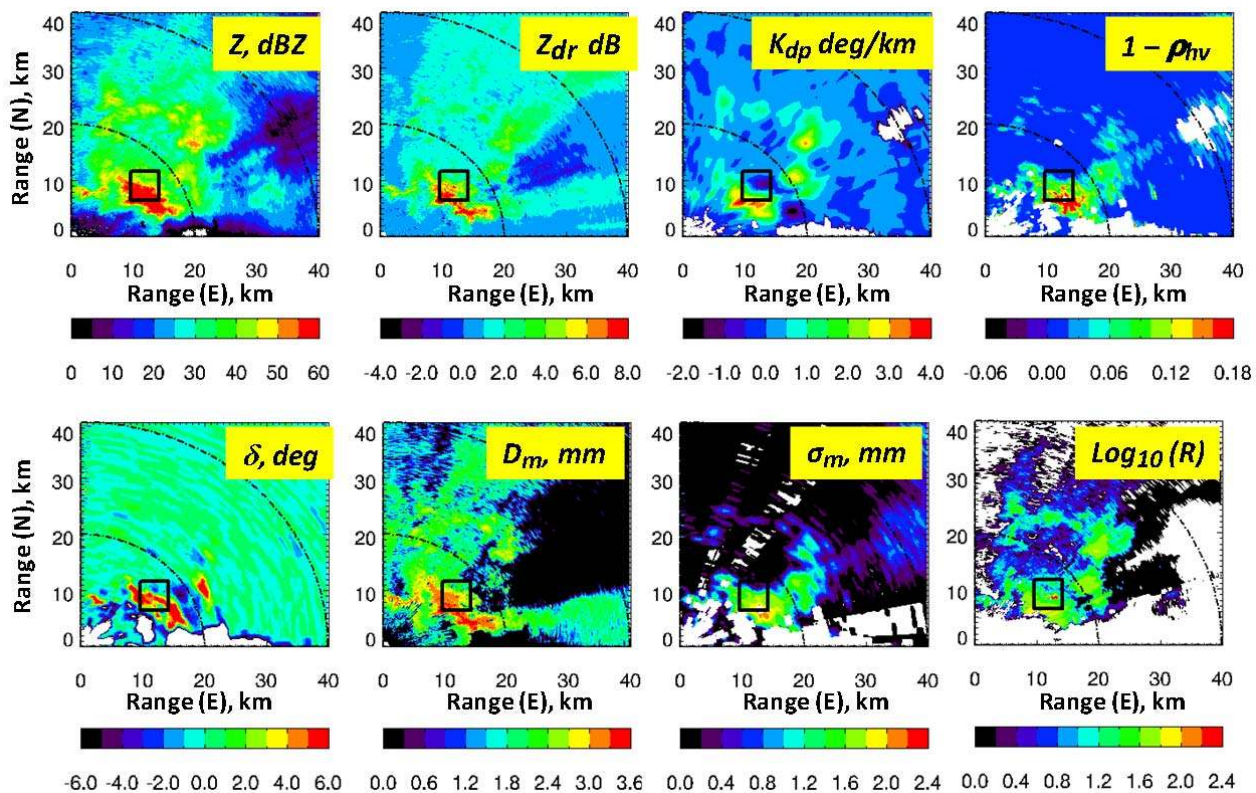


Fig. 13: ARMOR radar PPI scans (top panels) and retrieved DSD parameters and $\log(R)$ (mm/h) together with the estimated differential backscatter phase. The 2DVD site is marked with a black square.

3 D_{\max} Sampling issues

As alluded to earlier, the value of D_{\max} employed in deriving radar-rainfall relationships can produce significantly different results (Keenan et al. 2001), and the presence of large raindrops greatly influences attenuation-correction methods (the coefficient that relates specific attenuation and differential attenuation to K_{dp}) especially at C-band frequencies (Zrníc et al 2000; Carey et al. 2000; Keenan et al. 2001; Carey and Petersen 2014). The probability of recording large raindrops with a disdrometer is limited, largely due to sampling issues (Smith 1993) since the sensor area, for example of the JWD is only 50 cm² whereas for the 2DVD it is 100 cm².

When performing scattering simulations, either the measured DSD and the corresponding D_{\max} value can be used, or the measured DSD can be fitted with a gamma shape model and one can fix the ratio D_{\max}/D_m or D_{\max}/D_0 around 3 (D_0 is the median volume diameter) or one can use a DSD model with fixed $D_{\max}=8$ mm (e.g., Smith et al. 1993; Keenan et al. 2001; Gorgucci et al. 2002; Brangi et al. 2002). One way to increase our confidence in D_{\max} assumptions as well as improve our knowledge of large raindrop concentrations is to examine long-term measurements from well calibrated, side-by-side disdrometers that sample a variety of precipitation regimes.

Conveniently, in Huntsville, Alabama, there were two side-by-side 2DVD units (installed a few meters apart) as part of a long-term observation campaign from which over 7500 pair samples of temporally matched 1-minute DSD measurements were recorded by the two (frequently calibrated) 2D-video disdrometers, named SN16 and SN25 (operated by NASA). The measurement campaign was over a ten-month period, and included a variety of rain types and regimes. In a previous study (Thurai et al., 2014), the datasets had been used to examine DSD sampling issues and their impact on some of the DSD parameters such as D_m and σ_M . One example is given in Fig. 14 (a) which compares the D_m values from the matched 1-minute DSDs from the two 2DVDs. The comparisons are shown as a color intensity plot where the color scale indicates the number of occurrences on a log scale. The same datasets have been used for D_{\max} comparisons shown in Fig. 14 (b). Note however, D_{\max} values in the plot are ‘quantized’ with a resolution of 0.25 mm. As with the D_m comparisons, there seems relatively good correlation between the two sets of D_{\max} values, but the spread is, as expected, noticeably larger.

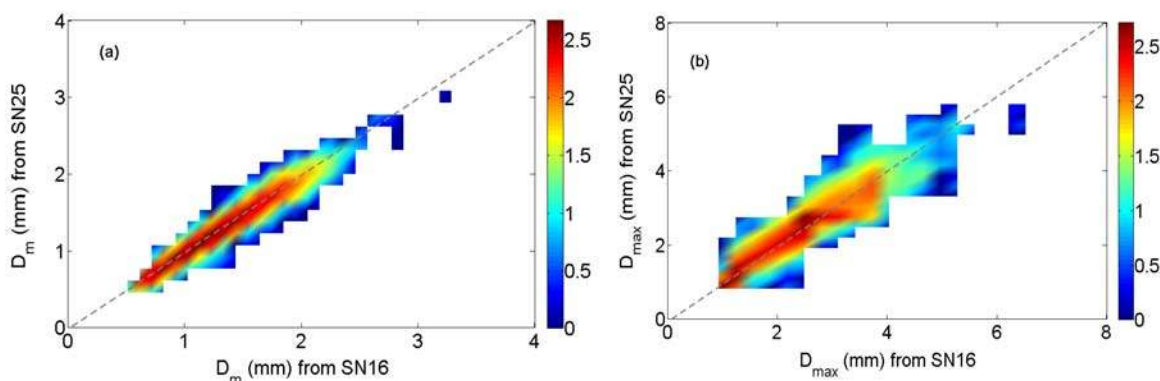


Fig. 14: (a) D_m and (b) D_{max} comparisons calculated using 1-minute DSDs from the two collocated 2DVDs in Huntsville.

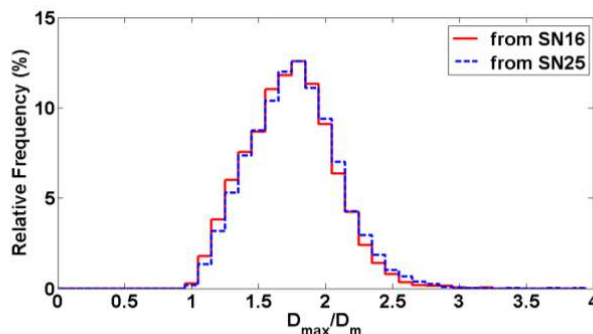
Table 2 summarizes the mean differences between the side-by-side measurements of D_{max} and their standard deviation for all the data, as well as for D_{max} values within several diameter intervals. The mean values of ΔD_{max} are very near zero, given the 0.25 mm ‘resolution’ of the 2DVD bins. However the standard deviation is *not* negligible, and furthermore, it increases with increasing D_{max} , reflecting the fact that larger drops are not well-sampled with the 100 cm² sensor area of the 2DVD (Smith, 1993). Note the integration time is 1-min. One would expect that increasing the integration time would reduce the standard deviation, as long as the ‘stationarity’ condition applies.

Table 2: Mean and standard deviations of the D_{max} comparisons from SN16 and SN25 for various D_{max} ranges.

D_{max} range	Mean(ΔD_{max})	Std. dev(ΔD_{max})	# of samples
All	0.04	0.40	7520
2 – 2.5 mm	0.03	0.48	3217
3 – 3.5 mm	-0.09	0.54	965
4 – 4.5 mm	-0.13	0.67	147
5 – 5.5 mm	-0.15	0.79	29

Of more interest is the ratio D_{max}/D_m and histograms determined from the 1-minute DSDs are shown in Fig. 15. The two curves represent the two separately derived histograms from SN16 and SN25. They show remarkable agreement. They also show that setting D_{max} to $3 \cdot D_m$ as the upper integration limit is sufficient to cover practically all cases. Note such histograms cannot be derived with many of the other disdrometers (e.g., Joss-Waldvogel type) because of the upper limit of drop size categories (often ~5-5.5 mm).

Fig. 15: Relative frequency of the ratio D_{max}/D_m determined from the 1-min DSDs from the two collocated 2DVDs. The number of samples = 7520 for each instrument (temporally matched DSDs).



4 Summary

Three events which produced very large drops have been investigated using 2DVD measurements and polarimetric radar observations. All three events had $D_{max} > 9$ mm. The first of these events – which occurred in Colorado – was an intense and relatively isolated rain cell with an echo top height of nearly 10 km. The CSU-CHILL S-band radar was set at fixed-pointing mode which enabled D_{max} at ground level to be correlated with Z_{dr} a few hundred m above ground level. Scattering calculations using the 1-minute DSDs show that excluding the 9 mm drop can result in somewhat lower values of Z_{hb} , Z_{dr} and K_{dp} at S, C and X bands, except for Z_{dr} at C-band (Mie region) which shows a small increase.

The second example occurred in Oklahoma and had produced the largest fully melted drop with a D_{eq} of 9.7 mm. A 3D reconstruction of the drop shape from the 2DVD-based contours was made from which a flattened base was very evident. A larger hydrometeor was also recorded during this mostly rain-dominated event, but its shape strongly suggests it was a melting hydrometeor (graupel/hail). The event was captured by the S-band operational weather radar as well as two X-band radars (and vertically-pointing Doppler profilers at Ku band and UHF). Analyses of the S band radar and one X band radar data show that K_{dp} values are much higher at X-band whereas Z_{dr} values are somewhat similar. These are corroborated by the 2DVD data-based scattering calculations which show similar D_m - Z_{dr} variation and very different R- K_{dp} variation.

The Huntsville event also had some melting hydrometeors, but it too was largely dominated by rain. The largest raindrop for this event had a D_{eq} of 9.1 mm. Nearby C-band polarimetric radar observations were made during this event as well. The D_m and σ_M values estimated from Z_{dr} and ρ_{hv} were in good agreement with those calculated from the 1-minute DSD during the time of the giant drop. Also found was significant differential backscatter phase in the very large drop region, which is to be expected at C-band due to resonance effects.

Finally, D_{max} sampling issues were addressed using 7500 minutes of temporally-matched DSDs from two collocated 2DVDs. High correlation was found between the two sets of DSDs in terms of D_m and D_{max} but the latter showed higher spread (and therefore higher fractional standard error). The spread was higher for DSDs containing high D_{max} values. Histograms of D_{max}/D_m showed that setting an upper integration limit of $D_{max}=3*D_m$ for scattering calculations using, for example gamma fitted DSDs is more 'realistic' than using a fixed value of say 8 mm.

Acknowledgements

The authors wish to thank the CHILL radar group from the Atmospheric Science Dept. at Colorado State University, in particular Patrick C. Kennedy, for supplying the CSU-CHILL radar data and providing information relating to the meteorological conditions associated with the Colorado event. Data collected by the X-band radar and 2DVD in Oklahoma were obtained from the Atmospheric Radiation Measurement (ARM) Program sponsored by the U.S. Department of Energy, Office of Science, Office of Biological and Environmental Research, Climate and Environmental Sciences Division. We would like to also thank Mary Jane Bartholomew for supplying the raw camera data from the DOE's 2DVD in Oklahoma and Dustin Phillips for maintaining the ARMOR radar in Huntsville, AL. Last, but not least, the authors would like to thank Dr. Walt Petersen for his collaboration and supplying NASA's 2DVD in Huntsville, AL, for side-by-side comparisons. MT and VNB acknowledge support from NASA Grant Award NNX10AJ12G as part of the Global Precipitation Mission – Ground Validation program.

References

- Ajayi, G. O., I. E. Owolabi** Rainfall parameters from disdrometer dropsize measurements at a tropical station, *Annales des Télécommunications*, Janvier–Fevrier 1987, Volume 42, Issue 1-2, pp 3-12,
- Atlas, D., R C. Srivastava, and R S. Sekkon**, 1973: Doppler radar characteristics of precipitation at vertical incidence. *Rev. Geophys. Space Phys.*, 2, 1–35.
- Atlas, D., C. W. Ulbrich, F. D. Marks Jr., E. Amitai, and C. R. Williams**. 1999. Systematic variation of drop size and radar–rainfall relation. *J. Geophys. Res* 104:6155–6169.
- Battan, L. J.**, Radar observation of the atmosphere, published by University of Chicago Press.
- Beard, K. V., C. Chuang**, 1987: A New Model for the Equilibrium Shape of Raindrops. *J. Atmos. Sci.*, 44, 1509–1524.
- Bringi, V.N. , Chandrasekar, V. , Meischner, P., Hubbert, J., Golestani, Y.**, 1991. Polarimetric radar signatures of precipitation at S- and C-bands. *IEE Proceedings F (Radar and Signal Processing)*, 138 (2), 109 – 119.
- Bringi, V. N., G-J Huang, V. Chandrasekar, E. Gorgucci**, 2002: A methodology for estimating the parameters of a gamma raindrop size distribution model from polarimetric radar data: Application to a squall-line event from the TRMM/Brazil campaign. *J. Atmos. Oceanic Technol.*, 19, 633–645.
- Bringi, V. N., V. Chandrasekar, J. Hubbert, E. Gorgucci, W. L. Randeu, M. Schoenhuber**, 2003: Raindrop Size Distribution in Different Climatic Regimes from Disdrometer and Dual-Polarized Radar Analysis. *J. Atmos. Sci.*, 60, 354–365.
- Brunkow, D., V. N. Bringi, P. C. Kennedy, S. A. Rutledge, V. Chandrasekar, E. A. Mueller, and R. K. Bowie**, 2000: A description of the CSU–CHILL National Radar Facility. *J. Atmos. Oceanic Technol.*, 17, 1596–1608.
- Bunkers, M. J.**, 2002: Vertical wind shear associated with left-moving supercells. *Wea. Forecasting*, 17, 845–855.

- Carey, L. D., S. A. Rutledge, D. A. Ahijevych, T. D. Keenan**, 2000: Correcting Propagation Effects in C-Band Polarimetric Radar Observations of Tropical Convection Using Differential Propagation Phase. *J. Appl. Meteor.*, 39, 1405–1433.
- Carey, L. D., and W. A. Petersen**, 2014: Sensitivity of C-band polarimetric radar-based drop size measurements to maximum diameter. *J. Appl. Meteor. Climatol.*, submitted.
- Gatlin, P.N., M. Thurai, V.N. Bringi, W.A. Petersen, D. Wolff, A. Tokay, L. Carey and M. Wingo**, 2014: Searching for large raindrops: A global summary of two-dimensional video disdrometer observations, Manuscript submitted.
- Gorgucci, E., V. Chandrasekar, V. N. Bringi, G. Scarchilli**, 2002: Estimation of Raindrop Size Distribution Parameters from Polarimetric Radar Measurements. *J. Atmos. Sci.*, 59, 2373–2384.
- Gunn, R., and G D. Kinzer**, 1949: The terminal velocity of fall for water droplets in stagnant air. *J. Meteor.*, 6, 243–248.
- Keenan, T. D., L. D. Carey, D. S. Zrnić, P. T. May**, 2001: Sensitivity of 5-cm Wavelength Polarimetric Radar Variables to Raindrop Axial Ratio and Drop Size Distribution. *J. Appl. Meteor.*, 40, 526–545.
- Kozu, T. Reddy, K. K. Mori, S., Thurai, M. Ong, J. T. Rao, D. N. Shimomai, T.**, 2006: Seasonal and Diurnal Variations of Raindrop Size Distribution in Asian Monsoon Region, *Journal of the Meteorological Society of Japan. Ser. II Special Issue: CPEA -Coupling Processes in the Equatorial Atmosphere- Vol. 84A*, 195-209.
- Matrosov, S. Y., R. Cifelli, P. C. Kennedy, S. W. Nesbitt, S. A. Rutledge, V. N. Bringi, B. E. Martner**, 2006: A Comparative Study of Rainfall Retrievals Based on Specific Differential Phase Shifts at X- and S-Band Radar Frequencies. *J. Atmos. Oceanic Technol.*, 23, 952–963.
- Notaros, B. M.**, 2008: Higher order frequency-domain computational electromagnetics. invited review paper, Special Issue on Large and Multiscale Computational Electromagnetics, *IEEE Trans. Antennas Propag.*, 56, 2251–2276.
- Otto, T., H. Russchenberg**, 2010, Estimation of the raindrop-size distribution at X-band using specific differential phase and differential backscatter phase, *Proc. 6th European Conf. on Radar in Meteorology and Hydrology: Adv. in Radar Technology*, Sibiu, Romania.
- Petersen, W. A., K. R. Knupp, D. J. Cecil, and J. R. Mecikalski**, 2007: The University of Alabama Huntsville THOR Center instrumentation: Research and operational collaboration, Preprints, 33rd Int. Conf. on Radar Meteorology, Cairns, Australia, *Amer. Meteor. Soc.*, 5.1.
- Rasmussen, R. M., A. J. Heymsfield**, 1987: Melting and Shedding of Graupel and Hail. Part I: Model Physics. *J. Atmos. Sci.*, 44, 2754–2763.
- Schönhuber, M., G. Lammer, and W. L. Randeu**, 2008: The 2D-video-distrometer. *Precipitation: Advances in Measurement, Estimation and Prediction*, S. Michaelides, Ed., Springer, 3–32.
- Sekeljac, N., A. Manic, E. Chobanyan, M. Thurai, V. N. Bringi, B. Notaros**, 2014: Electromagnetic Scattering by Oscillating Rain Drops of Asymmetric Shapes, *Proc. 2014 IEEE International Symposium on Antennas and Propagation and USNC-URSI Radio Science Meeting, July 6–11, 2014, Memphis, Tennessee, USA*.
- Smith, P. L., Z. Liu, J. Joss**, 1993: A Study of Sampling-Variability Effects in Raindrop Size Observations. *J. Appl. Meteor.*, 32, 1259–1269.
- Thurai, M., G. J. Huang, V. N. Bringi, W. L. Randeu, M. Schönhuber**, 2007: Drop Shapes, Model Comparisons, and Calculations of Polarimetric Radar Parameters in Rain, *J. Atmos. Oceanic Technol.*, 24, 1019–1032.
- Thurai, M., D. Hudak, V. N. Bringi**, 2008: On the Possible Use of Copolar Correlation Coefficient for Improving the Drop Size Distribution Estimates at C Band. *J. Atmos. Oceanic Technol.*, 25, 1873–1880.
- Thurai, M., C.R. Williams, V.N. Bringi**, 2014: Examining the correlations between drop size distribution parameters using data from two side-by-side 2D-video disdrometers, *Atmospheric Research, Volume 144*, 1 July 2014, Pages 95–110, Special Issue on Perspectives of Precipitation Science - Part II
- Thurai, M., V. N. Bringi, A. B. Manić, N. J. Šekeljić, and B. M. Notaroš**, 2014: Investigating rain drop shapes, oscillation modes, and implications for radiowave propagation, *Radio Science*, Revised manuscript submitted after minor revision.
- Tokay, A., and D. A. Short**, 1996: Evidence from tropical raindrop spectra of the origin of rain from stratiform versus convective clouds. *J. Appl. Meteor.*, 35, 355–371.
- Zrnić, D. S., T. D. Keenan, L. D. Carey, P. May**, 2000: Sensitivity Analysis of Polarimetric Variables at a 5-cm Wavelength in Rain. *J. Appl. Meteor.*, 39, 1514–1526.